Proceedings of the ASME 2010 3rd Joint US-European Fluids Engineering Summer Meeting and 8th International Conference on Nanochannels, Microchannels, and Minichannels
FEDSM-ICNMM2010
August 1-5, 2010, Montreal, Canada

FEDSM-ICNMM2010-30907

NUMERICAL SIMULATION OF A SYNTHETIC JET ACTUATOR USING A SIMPLIFIED PERIODIC BOUNDARY CONDITION

Antonio Pascau*
Fluid Mechanics Group and LITEC
CSIC-University of Zaragoza
Zaragoza, Spain 50018
Email: pascau@unizar.es

Nelson García
Fluid Mechanics Group and LITEC
CSIC-University of Zaragoza
Zaragoza, Spain 50018
Email: nelson@unizar.es

ABSTRACT

When using a collocated grid for the discretization of the unsteady Navier-Stokes equations special care has to be taken in the evaluation of the cell face velocity as if it is not properly calculated the resulting flow field may be dependent on the time step. This dependency increases as the time step is reduced so this problem can be of paramount importance in rapidly varying flows. As an illustration of the problem in a flow of industrial interest a synthetic jet has been chosen. Although the primary goal of the paper is not to compare computational and experimental results, the assessment with experimental data will highlight the discrepancies in the computational results with different time steps. For comparison purposes a well documented case was chosen: the first test case of the synthetic jet workshop organized by NASA in 2004, but with the new 2006 data. This flow is produced by a moving diaphragm at one of the sides of a cavity connected to an otherwise stagnant air through a slot. Near the slot exit the flow is almost bidimensional so in order to reduce computational time it has been modelled in a 2D domain with a transpiration velocity at the bottom boundary of a simplified cavity. This velocity tries to reproduce the waveform of the measurements at the slot exit with an appropriate combination of Fourier modes.

*Address all correspondence to this author.

NOMENCLATURE

- $A^u_{P|e,i}$ Diagonal coefficient of the momentum equation at e or i without the temporal contribution
- $\widetilde{A}^u_{P|e,i}$ Complete diagonal coefficient of the momentum equation at e or i
- u^* Velocity value at current iteration
- u^l Velocity value at previous iteration
- u^n Velocity value at preceding time step

INTRODUCTION

There is considerable interest in the potential use of synthetic jets to control the boundary layer separation under adverse pressure gradients. This type of flow is intrinsically time dependent and the interaction with the boundary layer is threedimensional in nature. However there are simplified experimental situations which possess the same features as the practical applications of synthetic jets while providing a very controlled flow which is basically two dimensional, thus amenable to be numerically explored with a reasonable number of turbulence models, grids and schemes without being discouraged by the turnover time. This relatively simple kind of flow is the one we have chosen to model. In particular we have studied the case 1 in the CFDVAL2004 workshop sponsored by NASA and other international organizations in 2004. This case refers to an isolated synthetic jet that issues into quiescent air. The flow is produced by a moving diaphragm driven by a piezolectric material in a cavity. The cavity is connected to open air through a slot with an aspect

ratio large enough to consider the flow to be twodimensional, at least in a region near the slot exit. The experimental setup and the geometry of the flow are described in a web page of NASA Langley Research Center as well as rather extensive velocity field data. Some time later a more documented (and seemingly more precise) set of data were included in the same web page. We have employed the latter in this study.

We specifically employed a collocated grid due to its coding simplicity. However, the ease of discretizing the equations, with only one grid for all variables, is at the cost of reducing the strength of the pressure velocity coupling. To couple the velocity and pressure fields in this type of grid a special interpolation procedure put forward by Rhie and Chow [1] is required. Our intention is to show that some adopted implementations of the Rhie-Chow procedure in transient flows can give rise to solutions dependent on the time step. This dependence has nothing to do with the discretization errors in the temporal term, in fact it is more pronounced when the time step is very small in relative terms, something that will be explained later. The inconsistency is due to the face velocity expression where some factors that contain the time step appear in the wrong places. To explain the link with the Rhie-Chow procedure that was originally put forward for steady calculations, a derivation of the face velocity expression in a transient case will be briefly explained. More details can be found in [2].

NUMERICAL BACKGROUND

In a collocated grid the face velocity does not satisfy a momentum equation, its field values are obtained with an appropriate average of some terms in the momentum equations at the nodes. For illustration purposes let us consider a generic interface e with two adjacent nodes E and P, all three along the x coordinate. The way to obtain the face expression is to write a fictitious discretized momentum equation at interface e formally identical to that at the nodes. Following the usual notation the equation both at nodes, $i = E, P$, and at face e is for a variable density case

$$A^u_{P|i,e}u^*_{i,e} = \sum_{j|i,e} A^u_j u^*_j + S^u_{i,e}\Delta V_{i,e} - \Delta V_{i,e}\left.\frac{\partial p}{\partial x}\right|^l_{i,e} + \\ + \frac{1-\alpha_u}{\alpha_u}\widetilde{A}^u_{P|i,e}(u^l_{i,e} - u^*_{i,e}) + \frac{\rho_{i,e}\Delta V_{i,e}}{\Delta t}(u^n_{i,e} - u^*_{i,e}) \quad (1)$$

with

$$\widetilde{A}^u_{P|i,e} = A^u_{P|i,e} + \frac{\rho_{i,e}\Delta V_{i,e}}{\Delta t} \qquad A^u_{P|i,e} = \sum_{j|i,e} A^u_j \quad (2)$$

$S^u_{i,e}$ is the source term for the x-momentum. $u^l_{i,e}$ is the value at the previous inner iteration and $u^n_{i,e}$ is the value at the preceding time step. These expressions are written for a general case where a transient calculation (real or pseudo) with a time step Δt is performed with underrelaxation (α_u). When the steady state is reached (if any) only the first line of Eqn. (1) remains. To derive the computable u_e expression a term in the fictitious e-equation is reformulated as an average of its nodal counterparts. After dividing Eqn. (1) by $A^u_{P|i,e}$ the original Rhie-Chow interpolation assumes that

$$H^u_e = \frac{\sum_{j|e} A^u_j u^*_j + S^u_e \Delta V_e}{A^u_{P|e}} = \overline{\left(\frac{\sum_{j|i} A^u_j u^*_j + S^u_i \Delta V_i}{A^u_{P|i}}\right)}^e = \overline{H^u_i}^e \quad (3)$$

This average term can be rewritten in terms of the average of the rest of the terms in the nodal equations. By doing so we end up with an expression for the face velocity that depends on the velocity field in the neighbourhood of e (at this iteration, at the previous one and at the preceding time step) and on the pressure field. The expression, named elsewhere as PICTURE [2], reads

$$(1+\delta_e)u^*_e = \overline{(1+\delta_i)u^*_i}^e + \alpha_u\Delta t\left[\overline{\frac{\delta_i}{\rho_i}\left.\frac{\partial p}{\partial x}\right|^l_i}^e - \frac{\delta_e}{\rho_e}\left.\frac{\partial p}{\partial x}\right|^l_e\right] + \\ + (1-\alpha_u)\left[(1+\delta_e)u^l_e - \overline{(1+\delta_i)u^l_i}^e\right] + \\ + \alpha_u\left[\delta_e u^n_e - \overline{\delta_i u^n_i}^e\right] \quad (4)$$

with

$$\delta_{e,i} = \frac{\rho_{e,i}\Delta V_{e,i}}{\Delta t A^u_{P|e,i}} \quad (5)$$

This expression is employed to estimate the new convecting velocities at the faces right after solving the momentum equation for the convected velocity. To obtain a field that satisfies continuity in each control volume a correction is derived following a SIMPLEC approach [3]. The velocity correction at the nodes is obtained as

$$(1+\delta_i)u'_i = -\alpha_u\Delta t\frac{\delta_i}{\rho_i}(1+\widetilde{k}_i)\left.\frac{\partial p}{\partial x}\right|'_i \quad (6)$$

where $\widetilde{k}_i$ is defined as

$$\widetilde{k}_i = \frac{\alpha_u\sum_{j|i}A^u_j}{\widetilde{A}^u_{P|i} - \alpha_u\sum_{j|i}A^u_j} = \frac{\alpha_u r_i}{1-\alpha_u r_i + \delta_i} \quad ; \quad r_i = \frac{\sum_{j|i}A^u_j}{A^u_{P|i}}$$

r_i is equal to one over most part of the domain except at the boundaries due to Dirichlet boundary conditions. The corresponding expression at the face e is

$$(1+\delta_e)u'_e = -\alpha_u \Delta t \left[\overline{\frac{\delta_i}{\rho_i} \widetilde{k}_i \left. \frac{\partial p}{\partial x} \right|_i'}^e + \frac{\delta_e}{\rho_e} \left. \frac{\partial p}{\partial x} \right|_e' \right] \tag{7}$$

Contrary to some previously employed SIMPLEC implementations this SIMPLEC procedure is consistent, that is, the correcting expression at the faces is the same whatever path is taken to calculate it, whether with the correction velocities at the nodes or with the correcting pressure field. The interested reader is referred to [3]. The SIMPLEC scheme applied to the pressure velocity coupling produces a pentadiagonal matrix in each coordinate that can be solved with a pentadiagonal matrix algorithm (PDMA).

Choi's suggestion on how to calculate the face velocity in a collocated grid for a general transient flow is [4]

$$u_e^* = \overline{u_i^*}^e + \alpha_u \Delta t \left[\overline{\frac{\delta_i}{\rho_i(1+\delta_i)} \left. \frac{\partial p}{\partial x} \right|_i}^e - \frac{\delta_e}{\rho_e(1+\delta_e)} \left. \frac{\partial p}{\partial x} \right|_e^l \right] + \\ + (1-\alpha_u) \left[u_e^l - \overline{u_i^l}^e \right] + \alpha_u \left[\frac{\delta_e}{1+\delta_e} u_e^n - \overline{\frac{\delta_i}{1+\delta_i} u_i^n}^e \right] \tag{8}$$

The distinction with respect to PICTURE is that Choi considers another term in the original momentum equation at e as that to be computed with an average of its nodal counterparts. This different starting point leads naturally to Eqn. (8). Choi defined H_e^u as

$$H_e^u = \frac{\sum_{j|e} A_j^u u_j^* + S_e^u \Delta V_e}{\widetilde{A}_{P|e}^u} = \overline{\left(\frac{\sum_{j|i} A_j^u u_j^* + S_i^u \Delta V_i}{\widetilde{A}_{P|i}^u} \right)}^e = \overline{H_i^u}^e \tag{9}$$

Note that the denominator of this expression is different from that of PICTURE. Here it is the complete diagonal term, $\widetilde{A}_{P|e}^u$, whereas in the case of PICTURE it was the term without the time factor, $A_{P|e}^u$. At the end of the iterative process within a time step PICTURE face velocity satisfies the transient discretized equation

$$(1+\delta_e)u_e^* = \overline{(1+\delta_i)u_i^*}^e + \overline{\frac{\Delta V_i}{A_{P|i}^u} \left. \frac{\partial p}{\partial x} \right|_i}^e - \frac{\Delta V_e}{A_{P|e}^u} \left. \frac{\partial p}{\partial x} \right|_e^l + \\ + \left[\delta_e u_e^n - \overline{\delta_i u_i^n}^e \right] \tag{10}$$

and if there is any steady state the final expression is

$$u_e^* = \overline{u_i^*}^e + \overline{\frac{\Delta V_i}{A_{P|i}^u} \left. \frac{\partial p}{\partial x} \right|_i}^e - \frac{\Delta V_e}{A_{P|e}^u} \left. \frac{\partial p}{\partial x} \right|_e^l$$

Contrary to PICTURE, Choi suggestion produces

$$(1+\delta_e)u_e^* = \overline{\Lambda_i(1+\delta_i)u_i^*}^e + \overline{\Lambda_i \frac{\Delta V_i}{A_{P|i}^u} \left. \frac{\partial p}{\partial x} \right|_i}^e - \frac{\Delta V_e}{A_{P|e}^u} \left. \frac{\partial p}{\partial x} \right|_e^l + \\ + \left[\delta_e u_e^n - \overline{\Lambda_i \delta_i u_i^n}^e \right] \tag{11}$$

and

$$u_e^* = \overline{\Lambda_i u_i^*}^e + \overline{\Lambda_i \frac{\Delta V_i}{A_{P|i}^u} \left. \frac{\partial p}{\partial x} \right|_i}^e - \frac{\Delta V_e}{A_{P|e}^u} \left. \frac{\partial p}{\partial x} \right|_e^l$$

where

$$\Lambda_i = \frac{1+\delta_e}{1+\delta_i} \tag{12}$$

Note that Λ_i contains a delta time factor and so makes both the transient and/or the steady solution dependent on the time step.

TURBULENCE MODELS

The k-ε model with Durbin's correction [5] to circumvent the problem of large kinetic energy values in regions of stagnating flow has ben used as the standard model in all computations. We also wanted to check the behavior of the Scale Adaptive Simulation (SAS) [6] but under the framework of the k-ε model, that is, we tried to verify if the SAS source term as proposed by Menter had the same scale adaptivity behavior in the k-ε model that in the Shear Stress Transport (SST) model. We used Menter's idea by setting up a model named k-ε-SAS in unsteady mode which includes in the ε equation a new term similar to that proposed by Menter for the SST-SAS model. This term contains the ratio between the turbulent length scale and the von Karman lenght scale. Especifically, this is

$$P_{SAS} = \xi P_k \frac{\varepsilon}{k} \frac{L}{L_{vk}} \tag{13}$$

ξ is a model constant and P_k is the production term of kinetic energy. The lenghts involved are

$$L = \frac{k^{3/2}}{\varepsilon} \quad ; \quad L_{vk} = \frac{S}{U''} \quad ; \quad U'' = \sqrt{\frac{\partial^2 u_i}{\partial x_j \partial x_j} \frac{\partial^2 u_i}{\partial x_k \partial x_k}} \tag{14}$$

S being the second invariant of the mean rate-of-strain tensor. The effect of this term is to increase the levels of the dissipation rate of kinetic energy and hence to reduce the turbulent viscosity. By doing so when the equations are run in unsteady mode flow structures of smaller size can be observed as the turbulent Reynolds number is also reduced. When including SAS new term the time step acts as a kind of average factor in such a way that when moving to large time steps k-epsilon standard results are recovered. The results obtained with this model were indistinguishable from those of Durbin's k-ε for all cases tested. We must note that no perturbation of the transpiration velocity was introduced because we deemed that the shear layer at the slot exit would act as the trigger mechanism to develop the SAS-related turbulent structures [7]. As the flow strongly contracts at the slot and the particular turbulent details of the flow inside the cavity seem to be of minor importance there is no point in perturbing the boundary condition wave.

RESULTS

In Fig.1 the domain utilized in the computational experiments is presented. The grid was 68x490 with 14 nodes inside the slot and an expansion ratio of 1.2 towards the lateral boundaries. The domain size was 40dx40d, d=1.27 mm being the slot width. In all the open flow boundaries a zero gradient boundary condition was employed for all variables. The cavity where the piezoelectric device was located was simulated with a simple rectangular domain. A combination of 5 Fourier modes was neccesary for matching the computational velocity and the experimental profile at $y = 0$, the slot exit, along one cycle. This velocity wave was imposed at the bottom boundary of the cavity, downscaled by the slot-to-cavity width ratio. At every time step some relaxed subiterations were carried out, stopping when the residual was below 10^{-4} for both momentum equations and 10^{-3} for the continuity equation at each time step.

The residual for the u-velocity is defined as

$$res_u = \frac{\left(\sum_i \left|\widetilde{A}^u_{P|i}u_i - \sum_{j|i} A^u_j u_j - S^u_i \Delta V_i + \Delta V_i \left.\frac{\partial p}{\partial x}\right|_i - \frac{\rho_i \Delta V_i}{\Delta t} u^n_i\right|^2\right)^{1/2}}{\left(\sum_i \left|\widetilde{A}^u_{P|i}u_i\right|^2\right)^{1/2}} \tag{15}$$

Likewise, a residual for the υ-velocity can be defined, res_υ. The mass imbalance is calculated as

$$res_m = \frac{(\sum_i |(\rho_e u^*_e - \rho_w u^*_w)\Delta y + (\rho_n \upsilon^*_n - \rho_s \upsilon^*_s)\Delta x|)}{(\sum_i inflow_i)} \tag{16}$$

$inflow_i$ refers to the mass flow coming into a cell.

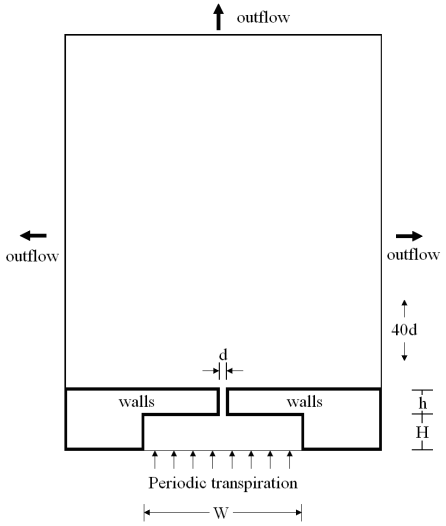

FIGURE 1. Computational domain with specified boundary conditions

The time step employed is $1.5\,10^{-6}$. Being 445Hz the frequency of the piezoelectric device used in the experiments that time interval means approximately 1500 time steps per cycle or a time step every 0.25^o of phase angle. The run was started from scratch to obtain a preliminary solution at 90^o phase angle, then ten complete cycles were run and the results of the eleventh cycle were stored. An a posteriori check was carried out to ensure that there was no significant change in the field variables in subsequent cycles.

Figures 2 and 3 show the comparison between measured and computed flow fields at 90^o and 270^o phase angles with PICTURE. The first one is a bit ahead of the point of maximum ejection velocity and the second one is also close to the point of maximum suction velocity. As can be seen in Fig. 2 the flow pattern is very well reproduced by the computations, although the peak velocity and the region where υ velocity attains large values is less wide. The prediction at 270^o phase angle is somehow better and the distribution of relative values is very similar in both graphs. All results presented are independent of the time step. There have been some previous researchers who have calculated the same flow. Our results are comparable to those of Vatsa and Turkel [8] which are the ones that showed the best performance.

The main finding of this work relates to the bad use of cell face velocity calculation in collocated grids in transient cases. We performed several test cases with different time steps in order to vary δ_i and produce significant changes in Λ_i when using Choi's approach in Eqn. 11.

In Fig. 4 a direct comparison between the computed results with Choi's approach obtained with the baseline time step ($1.5\,10^{-6}$) and another time step two orders of magnitude smaller

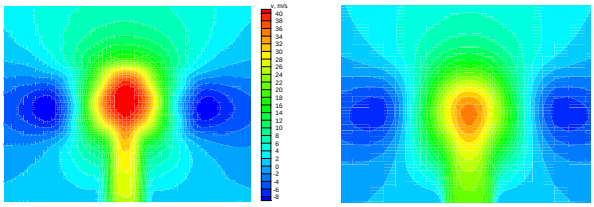

FIGURE 2. Comparison of measured and computed v velocity at 90^o phase angle.

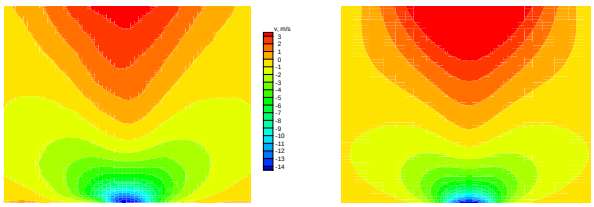

FIGURE 3. Comparison of measured and computed v velocity at 270^o phase angle.

is depicted. The solution with the smaller time step was obtained as follows: we started with the baseline solution, ran the program for three cycles and stored the solution of the fourth one. The a posteriori check was also performed.

An image is worth one thousand words. The effect of an incorrect calculation of the face velocity is to make the solution dependent on the time step as the pictures unmistakably show.

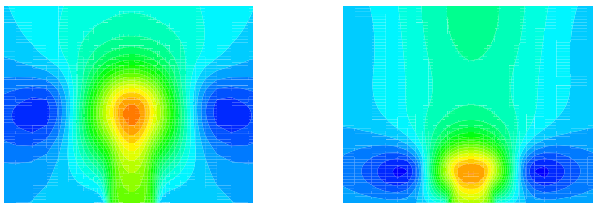

FIGURE 4. Comparison of computed v velocities at 90^o phase angle with two different time steps.

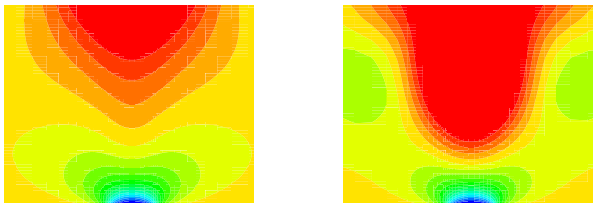

FIGURE 5. Comparison of computed v velocities at 270^o phase angle with two different time steps.

CONCLUSIONS

In this paper a comparison of the results obtained in a transient flow with inconsistent treatment of the face velocity has been presented. The approach proposed by Choi, that has been profusely utilized in the literature, can produce substantial differences in the flow pattern depending on the adopted time step. If a consistent approximation is employed all results are the same, irrespective of the time step.

ACKNOWLEDGMENT

This work was supported in part by Programme AlBan of European Commission Delegations in Latin America (Grant E06D103621VE).

REFERENCES

[1] Rhie, C. M., and Chow, W. L., 1983. "Numerical Study of the Turbulent Flow Past an Airfoil with Trailing Edge Separation". *AIAA Journal,* ***21***(11), pp. 1525–1532.

[2] Pascau, A. "Cell Face Velocity Alternatives in a Structured Collocated Grid for the Unsteady Navier-Stokes Equations". *International Journal for Numerical Methods in Fluids. Accepted for publication. Early view.*

[3] Pascau, A., and García, N., 2010. "Consistency of SIMPLEC Scheme in Collocated Grids". In Proceedings ECCOMAS Computational Fluid Dynamics Conference, CFD2010, J. C. F. Pereira, ed., ECCOMAS.

[4] Choi, S. K., 1999. "Note on the Use of Momentum Interpolation Method for Unsteady Flows". *Numerical Heat Transfer, Part A,* ***36***, pp. 545–550.

[5] Durbin, P. A., 1996. "On the k-ε Stagnation Point Anomaly". *International Journal of Heat and Fluid Flow,* ***17***, pp. 89–90.

[6] Menter, F. R., and Egorov, Y., 2005. "A Scale-Adaptive Simulation Model using Two-Equation Models". In 43rd AIAA Aerospace Sciences Meeting and Exhibit, 10-13 January 2005, Reno, Nevada, AIAA. Paper number 2005–1095.

[7] Davidson, L., 2006. "Evaluation of the SST-SAS Model: Channel Flow, Axymmetric Diffuser and Axi-Symmetric Hill". In European Conference on Computational Fluid Dynamics, Delft, The Netherlands, ECCOMAS.

[8] Vatsa, V. N., and Turkel, E., 2006. "Simulation of Synthetic Jets Using Unsteady Reynolds-Averaged Navier-Stokes Equations". *AIAA Journal,* ***44***(2), pp. 217–224.